Supporting Information

one-year real-time measurement of black carbon in the rural area of Qingdao, Northeastern China: seasonal variations, meteorological effects, and the COVID-19 case analysis

Shijie Cui [1], Jiukun Xian [1], Fuzhen Shen [1], Lin Zhang [1], Baoling Deng[1], Yunjiang Zhang [1,*], Xinlei Ge [1]

1 Jiangsu Key Laboratory of Atmospheric Environment Monitoring and Pollution Control, Collaborative Innovation Center of Atmospheric Environment and Equipment Technology, School of Environmental Sciences and Engineering, Nanjing University of Information Science and Technology, Nanjing 210044, China; csj930429@163.com (S.C.), jiukun_xian@163.com (J.X.), 20161119082@nuist.edu.cn (F.S.), zhanglin199455@163.com (L.Z.), baoling_deng@163.com (B.D.), caxinra@163.com (X.G.), yjzhang@nuist.edu.cn (Y.Z.)

* Correspondence: yjzhang@nuist.edu.cn; Tel.: +86-15850726433 (Y.Z.)

Figure S1. Sampling site location and its surroundings.

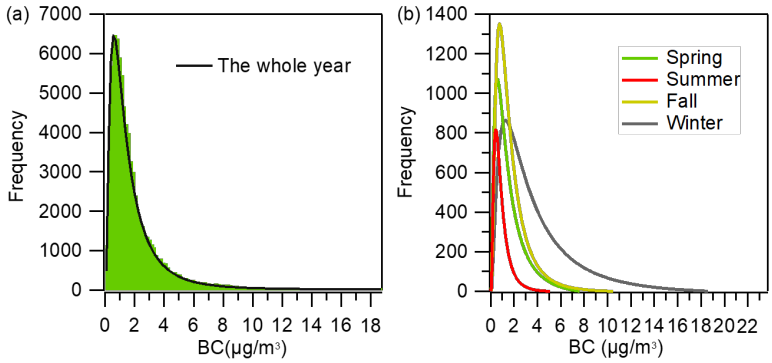

Figure S2: The distribution of BC concentrations in the whole year (a) (the green bar is the number of BC concentrations within an interval of 0.05 μg m^{-3}, the black line is the fitted curve following a lognormal function), and four seasons (b).

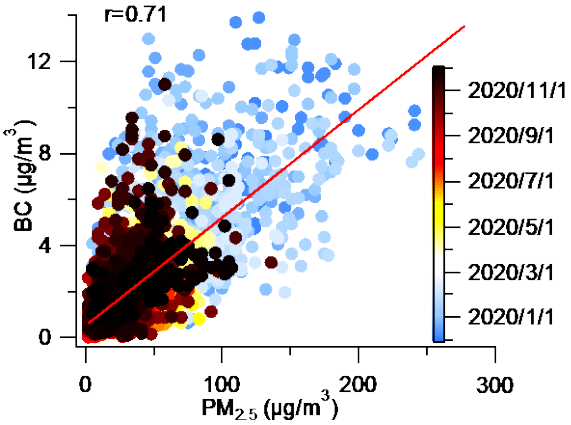

Figure S3. Scatter plot of BC vs. $PM_{2.5}$, the red line in the graph is the fitted line, and the scatter color represents the date.

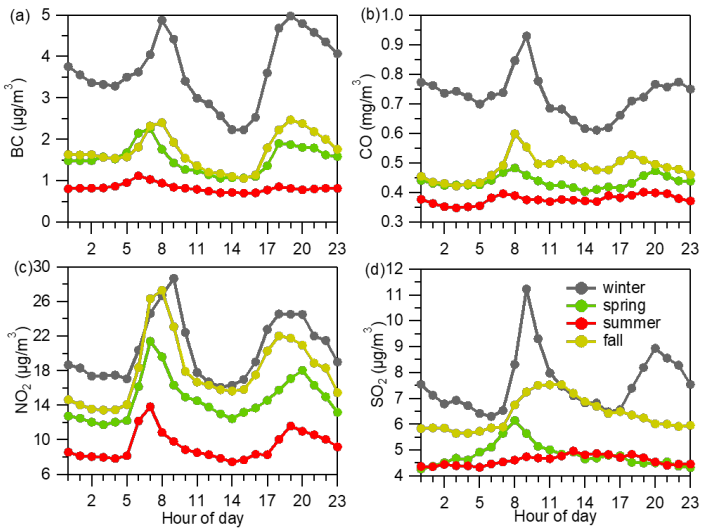

Figure S4. Diurnal pattern of BC (a), CO (b), NO_2 (c), and SO_2 (d) in four seasons over the whole campaign period.

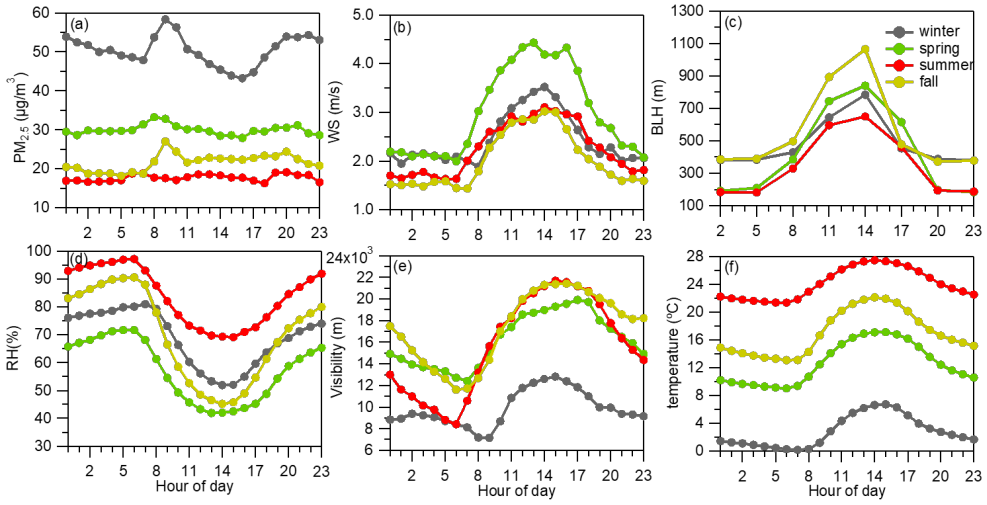

Figure S5: Diurnal patterns of average $PM_{2.5}$ concentration (a), wind speed (WS) (b), boundary layer height (BLH) (c), relative humidity (RH) (d), visibility (e), and temperature (T) (f) in four seasons.

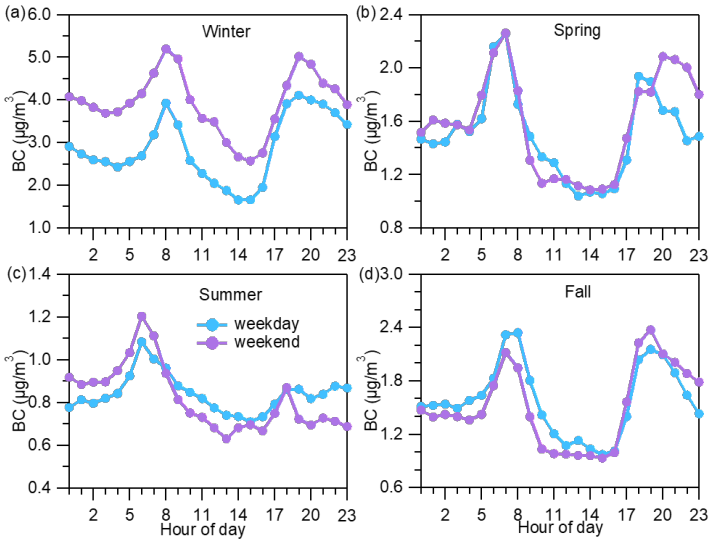

Figure S6. Diurnal patterns of average BC concentrations during weekdays and weekends in four seasons.

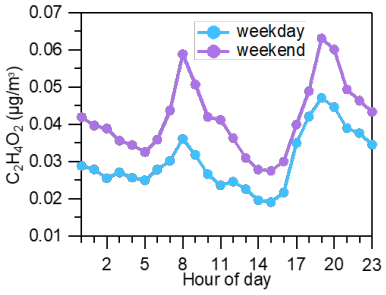

Figure S7. Diurnal patterns of average $C_2H_4O_2$ concentrations during weekdays and weekends. The tracer $C_2H_4O_2$ for biomass combustion is derived from organic fragments measured by Aerodyne soot particle aerosol mass spectrometer (SPAMS), which is installed at the same location as MAAP, from November 25, 2019, to January 7, 2020.

Table S1. Results of some long-term measurements of BC concentrations (μg m^{-3}) in East Asia

Site	Site type	Time	Conc.	Instrument	References
Qingdao	Rural	2019.12-2019.11	1.92±1.89	MAAP 5012[1]	This study
Beijing, China	Urban	2005-2013	4.3	-	[1]
Beijing, China	Urban	2015.1-2017.12	3.5	AE-31 [2]	[2]
Beijing, China	Rural	2014.1-2015.1	4.4 ± 3.7	AE-31 [2]	[3]
Baoji, China	Urban	2015.01-2015.12	2.9±1.7	AE-31 [2]	[4]
Xianghe, China	Suburban	2013.04-2015.03	5.39±4.44	AE-31 [2]	[5]
Hefei, China	Urban	2012.06-2013.05	3.5±2.5	AE-31 [2]	[6]
Wuhan, China	Urban	2014.11-2016.11	3.01±1.97	AE-31 [2]	[7]
Nanjing, China	Suburban	2017.12-2018.11	2.78±1.96	MAAP 5012[1]	[8]
Shanghai, China	Urban	2017.1-2017.12	2.19 ±1.73	AE-33 [3]	[9]
Xiamen, China	Urban	2014.1-2014.12	4.27 ±1.88	AE31 [2]	[10]
Guangzhou, China	Urban	2007.12-2008.12	4.7	AE-31 [2]	[11]
Dianshan Lake, China	Remote	2014.2-2019.2	1.39±1.15	AE-31 [2]	[12]
Byeongcheon, Korea	Rural	2012.4-2012.9	1.43	MAAP 5012[1]	[13]
Manora Peak, Central Himalayas	Remote	2004.11-2007.12	0.99±0.02	AE-42[4]	[14]
Fukue Island, Japan	Remote	2009.4-2015.3	0.36	COS-MOS[5]	[15]
Darjeeling, India	Urban	2009.1-2015.12	3.40±0.7	AE 52[6]	[16]
Delhi, India	Rural	2015.4-2016.3	7.2±0.3	AE-42 [4]	[17]
Pune, India	Urban	2018.4-2019.2	3.9±2.8	AE-33 [3]	[18]
Mahabaleshwar, India	Rural	2018.4-2019.2	1.4±0.9	AE-33 [3]	

[1] Multi-spectrum carbon monitor (Model BC 1054). [2] Aethalometer (Model AE-31 Magee Scientific, USA). [3] Aethalometer (Model AE-33 Magee Scientific, USA). [4] Aethalometer (Model AE-42 Magee Scientific, USA). [5] Continuous soot-monitoring system. [6] Aethalometer (Model AE-52 Magee Scientific, USA).

References

1. Chen, Y.; Schleicher, N.; Fricker, M.; Cen, K.; Liu, X.L.; Kaminski, U.; Yu, Y.; Wu, X.F.; Norra, S. Long-term variation of black carbon and PM2.5 in Beijing, China with respect to meteorological conditions and governmental measures. *Environ. Pollut.* **2016**, *212*, 269-278, doi:10.1016/j.envpol.2016.01.008.
2. Xia, Y.; Wu, Y.; Huang, R.J.; Xia, X.; Tang, J.; Wang, M.; Li, J.; Wang, C.; Zhou, C.; Zhang, R. Variation in black carbon concentration and aerosol optical properties in Beijing: Role of emission control and meteorological transport variability. *Chemosphere* **2020**, *254*, 126849, doi:10.1016/j.chemosphere.2020.126849.
3. Ji, D.; Li, L.; Pang, B.; Xue, P.; Wang, L.; Wu, Y.; Zhang, H.; Wang, Y. Characterization of black carbon in an urban-rural fringe area of Beijing. *Environ. Pollut.* **2017**, *223*, 524-534, doi:10.1016/j.envpol.2017.01.055.
4. Zhou, B.; Wang, Q.; Zhou, Q.; Zhang, Z.; Wang, G.; Fang, N.; Li, M.; Cao, J. Seasonal Characteristics of Black Carbon Aerosol and its Potential Source Regions in Baoji, China. *Aerosol Air Qual. Res.* **2018**, *18*, 397-406, doi:10.4209/aaqr.2017.02.0070.
5. Ran, L.; Deng, Z.Z.; Wang, P.C.; Xia, X.A. Black carbon and wavelength-dependent aerosol absorption in the North China Plain based on two-year aethalometer measurements. *Atmos. Environ.* **2016**, *142*, 132-144, doi:10.1016/j.atmosenv.2016.07.014.
6. Zhang, X.; Rao, R.; Huang, Y.; Mao, M.; Berg, M.J.; Sun, W. Black carbon aerosols in urban central China. *J. Quant. Spectrosc. Radiat. Transfer* **2015**, *150*, 3-11, doi:10.1016/j.jqsrt.2014.03.006.
7. Liu, B.; Ma, Y.; Gong, W.; Zhang, M.; Shi, Y. The relationship between black carbon and atmospheric boundary layer height. *Atmos. Pollut. Res.* **2019**, *10*, 65-72, doi:10.1016/j.apr.2018.06.007.
8. Zhang, L.; Shen, F.; Gao, J.; Cui, S.; Yue, H.; Wang, J.; Chen, M.; Ge, X. Characteristics and potential sources of black carbon particles in suburban Nanjing, China. *Atmos. Pollut. Res.* **2020**, *11*, 981-991, doi:10.1016/j.apr.2020.02.011.
9. Wei, C.; Wang, M.H.; Fu, Q.Y.; Dai, C.; Huang, R.; Bao, Q. Temporal Characteristics and Potential Sources of Black Carbon in Megacity Shanghai, China. *J. Geophys. Res.-Atmos.* **2020**, *125*, doi:10.1029/2019jd031827.
10. Deng, J.; Zhao, W.; Wu, L.; Hu, W.; Ren, L.; Wang, X.; Fu, P. Black carbon in Xiamen, China: Temporal variations, transport pathways and impacts of synoptic circulation. *Chemosphere* **2020**, *241*, 125133, doi:10.1016/j.chemosphere.2019.125133.
11. Chen, X.; Zhang, Z.; Engling, G.; Zhang, R.; Tao, J.; Lin, M.; Sang, X.; Chan, C.; Li, S.; Li, Y. Characterization of fine particulate black carbon in Guangzhou, a megacity of South China. *Atmos. Pollut. Res.* **2014**, *5*, 361-370, doi:10.5094/apr.2014.042.
12. Jia, H.; Huo, J.; Fu, Q.; Duan, Y.; Lin, Y.; Xue, H.; Fan, L.; Cheng, J. Atmospheric characteristics and population exposure assessment of black carbon at a regional representative site in the Yangtze River Delta region, China based on the five-year monitoring. *Sci. Total Environ.* **2021**, 145990, doi:10.1016/j.scitotenv.2021.145990.
13. Lee, J.; Yun, J.; Kim, K.J. Monitoring of black carbon concentration at an inland rural area including fixed sources in Korea. *Chemosphere* **2016**, *143*, 3-9, doi:10.1016/j.chemosphere.2015.04.003.
14. Dumka, U.C.; Moorthy, K.K.; Kumar, R.; Hegde, P.; Sagar, R.; Pant, P.; Singh, N.; Babu, S.S. Characteristics of aerosol black carbon mass concentration over a high altitude location in the Central Himalayas from multi-year measurements. *Atmos. Res.* **2010**, *96*, 510-521, doi:10.1016/j.atmosres.2009.12.010.
15. Kanaya, Y.; Pan, X.; Miyakawa, T.; Komazaki, Y.; Taketani, F.; Uno, I.; Kondo, Y. Long-term observations of black carbon mass concentrations at Fukue Island,western Japan, during 2009–2015: constraining wet removal rates and emission strengths from East Asia. *Atmos. Chem. Phys.* **2016**, *16*, 10689-10705, doi:10.5194/acp-16-10689-2016.
16. Sarkar, C.; Roy, A.; Chatterjee, A.; Ghosh, S.K.; Raha, S. Factors controlling the long-term (2009-2015) trend of PM2.5 and black carbon aerosols at eastern Himalaya, India. *Sci. Total Environ.* **2019**, *656*, 280-296, doi:10.1016/j.scitotenv.2018.11.367.
17. Dumka, U.C.; Kaskaoutis, D.G.; Devara, P.C.S.; Kumar, R.; Kumar, S.; Tiwari, S.; Gerasopoulos, E.; Mihalopoulos, N. Year-long variability of the fossil fuel and wood burning black carbon components at a rural site in southern Delhi outskirts. *Atmos. Res.* **2019**, *216*, 11-25,

doi:10.1016/j.atmosres.2018.09.016.

18. Meena, G.S.; Mukherjee, S.; Buchunde, P.; Safai, P.D.; Singla, V.; Aslam, M.Y.; Sonbawne, S.M.; Made, R.; Anand, V.; Dani, K.K., et al. Seasonal variability and source apportionment of black carbon over a rural high-altitude and an urban site in western India. *Atmos. Pollut. Res.* **2021**, *12*, 32-45, doi:10.1016/j.apr.2020.10.006.